

# Microencapsulated paraffin as a tribological additive for advanced polymeric coatings

Reza GHEISARI<sup>1</sup>, Mariela VAZQUEZ<sup>2</sup>, Vasilis TSIGKIS<sup>1</sup>, Ali ERDEMIR<sup>1</sup>, Karen L. WOOLEY<sup>2,3,4</sup>, Andreas A. POLYCARPOU<sup>1,\*</sup>

<sup>1</sup> J. Mike Walker '66 Department of Mechanical Engineering, Texas A&M University, College Station 77843, USA

<sup>2</sup> Department of Chemistry, Texas A&M University, College Station 77843, USA

<sup>3</sup> Department of Materials Science & Engineering, Texas A&M University, College Station 77843, USA

<sup>4</sup> Department of Chemical Engineering, Texas A&M University, College Station 77843, USA

Received: 11 September 2022 / Revised: 27 November 2022 / Accepted: 20 December 2022

© The author(s) 2022.

**Abstract:** Numerous tribological applications, wherein the use of liquid lubricants is infeasible, require adequate dry lubrication. Despite the use of polymers as an effective solution for dry sliding tribological applications, their poor wear resistance prevents the utilization in harsh industrial environment. Different methods are typically implemented to tackle the poor wear performance of polymers, however sacrificing some of their mechanical/tribological properties. Herein, we discussed the introduction of a novel additive, namely microencapsulated phase change material (MPCM) into an advanced polymeric coating. Specifically, paraffin was encapsulated into melamine-based resin, and the capsules were dispersed in an aromatic thermosetting co-polyester (ATSP) coating. We found that the MPCM-filled composite exhibited a unique tribological behavior, manifested as “zero wear”, and a super-low coefficient of friction (COF) of 0.05. The developed composite outperformed the state-of-the-art polytetrafluoroethylene (PTFE)-filled coatings, under the experimental conditions examined herein.

**Keywords:** microencapsulated phase change material (MPCM); friction reduction additive; advanced polymeric coating

## 1 Introduction

Polymers are consistently growing as tribologically viable materials especially under dry sliding conditions, such as those experienced in space applications. They provide notably advantageous properties such as easy machinability, reasonable production cost, and light weight, as well as outstanding unique characteristics such as excellent corrosion resistance. Nonetheless, their poor wear resistance and friction properties hinder their more prevalent utilization in industrial applications. To tackle such shortcomings, three major approaches have been adapted, namely compounding polymers with other lubricious polymers/lamellar

solids [1–3], adding fillers such as fibers, oxides, and metallic nanoparticles [4, 5], and incorporating encapsulated additives such as ionic liquids (ILs) and paraffins [6, 7]. The difference between ILs and other fillers is that they need to be properly encapsulated in a core–shell structure before blending with the polymer matrix. A brief description of the advantages and disadvantages of these categories is presented below.

Among lubricious polymeric additives [1, 8], polytetrafluoroethylene (PTFE) has been widely investigated and utilized by numerous researchers and industries. The unique molecular structure and chemical composition of PTFE result in minimal

\* Corresponding author: Andreas A. POLYCARPOU, E-mail: apolycarpou@tamu.edu

friction between its polymeric chains due to the fluorophilic polymer interchain interactions. In addition, PTFE can also serve as a polymeric matrix to accommodate other fillers, e.g., polyamide-imide (PAI) and polyether ether ketone (PEEK) [9, 10]. In fact, under certain conditions, dry sliding can yield a coefficient of friction (COF) of 0.06 in PEEK-filled PTFE composites, which epitomizes the frictional characteristics of PTFE [10]. However, it is sometimes neglected that obtaining such a low COF is limited to linearly reciprocating motion and certain experimental parameters. In addition, because PTFE is chemically inert, it cannot be cross-linked, yielding poor creep and wear resistance, and therefore a controlled amount of filler has to be incorporated to enhance the tribological performance [11]. When PTFE is being used as a filler, e.g., in advanced polymeric coatings, it exhibits enhanced tribological attributes, manifested as “zero wear” and low COFs, at ca. 0.2 under ambient conditions [3, 12, 13]. While the wear resistance of PTFE-filled composites can be tuned with the appropriate selection of the supportive polymeric matrix, e.g., aromatic thermosetting co-polyester (ATSP), a further reduction in COF ( $< 0.1$ ) will require additional modifications of the additive composite. In general, the effective lubricating mechanisms of composite materials are based on lowering the shear resistance of the composite material and/or generating a lubricious transfer film on the countersurface.

Another category of fillers, which has been widely experimented and successfully implemented, is particulate additives, mostly in the form of non-organic fillers, including and not limited to metals, minerals, and oxides and graphitic compounds (e.g., copper, silicon carbide, and graphite oxide). These particles are generally used for fortifying the wear resistance of the polymers; thus, it is common to produce hybrid polymer–composite films, which include the polymer matrix in addition to particulate fillers. References [7, 8] have investigated the role of the chemical composition, particle size, volume fraction, shape, and specific surface area of these particles on enhancing the tribological performance of the polymer composites. In fact, the nanoparticles seem to be more effective in enhancing the mechanical and tribological properties of the polymers, since lower volume fraction results

in better modifications when compared to similar microparticles [1, 9]. The lowest COF and wear rate were reported for bronze particles and carbon fiber fillers added into PTFE matrix, which yielded 0.39 and  $2.25 \times 10^{-6}$  mm<sup>3</sup>/(N·m), respectively [1]. The emergence of hybrid composites has introduced novel fiber/particulate fillers, which could provide further tribological improvements [14, 15], yet at high raw material and production costs. The other shortcoming of such filled polymers is the weak interfacial interactions between the additives and the polymeric matrix, which result in inhomogeneous mechanical strength and consequently wear of the composite polymer.

The last category of fillers, which has not been extensively investigated, is micro-/nano-encapsulated additives. Encapsulation of the additives facilitates their embedment in a polymeric matrix, which would have been impossible otherwise. This area of research initiated by implementing ILs as core materials, which are room-temperature stable molten salts, encompassed in a polymeric shell to embed this lubricious liquid lubricant in a solid polymeric matrix. ILs enhance tribological properties of a base lubricant in the form of friction and wear reduction. Such enhancements on a metallic surface were obtained via generating a tribo-film on the sliding surfaces through adsorption. Microencapsulated 1-hexyl-3-methylimidazolium bis(trifluoromethyl sulphonyl) imide ([HMIM][NTf<sub>2</sub>]) IL was integrated into the top layer of a PTFE lubricious coating at 5 wt% [6]. Tests conducted under dry sliding conditions on both unfilled and filled polymer composites demonstrated lower wear and COFs. The obtained experimental data revealed that the IL could provide a 12% COF reduction, and up to a 70% decrease in the wear rate for hollow microcapsule IL cores. Reference [7] investigated the effect of the embedment of wax lubricant capsules into an epoxy on the tribological performance of the composite, and a dramatic decrease of the friction and wear with the increasing wax content was reported. Microencapsulated phase change materials (MPCMs) are another category of lubricious fillers that can be integrated in the matrix through an encapsulation process and has yet to be explored.

The objective of the present study is to introduce and preliminarily investigate the potential for MPCMs as effective and efficient additives for polymeric coatings in realistic operational conditions in dry contacts. We have demonstrated the enhancement in the tribological performance of an advanced bearing polymer, namely ATSP via implementing MPCM, and showed its superior performance compared to PTFE as a state-of-the-art industry-leading additive for solid lubrication.

## 2 Materials and methods

### 2.1 Materials

Shoe pins in the shape of half ellipsoids were made from SAE 52100 bearing steel. The exact chemical compositions of 52100 steel, as provided by the manufacturer, are shown in Table S1 in the Electronic Supplementary Material (ESM)). The flat side with a diameter ( $d_p$ ) of 10.9 mm and root-mean-square (RMS) roughness of 0.1  $\mu\text{m}$  was in contact with the disk. Disks with a diameter ( $d_D$ ) of 50.8 mm and thickness of 5 mm were machined out of O1 tool steel, as shown in Fig. 1. They were then blasted with silicon carbide grit, with an average size of 250–300  $\mu\text{m}$ , to enhance the bonding between the coating and substrate. The RMS roughness of the sandblasted substrates was  $5.46 \pm 0.08 \mu\text{m}$ . The disks were coated with 0, 10, and 20 wt% MPCM filler in an ATSP polymeric matrix, resulting in Coatings A0, A2, and A3, respectively. Coating A1 was used to compare the effect of MPCM filler on reducing the friction and wear and the commonly used PTFE filler, as shown in Table 1. A composition of 5 wt% PTFE filler was chosen

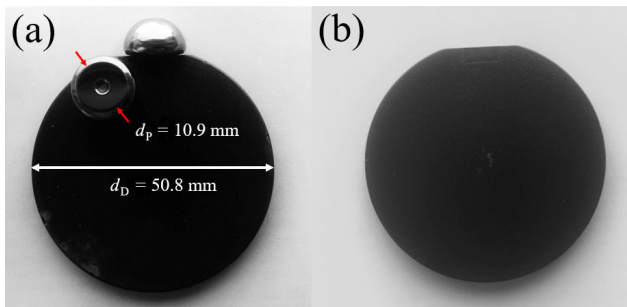


**Fig. 1** (a) Neat ATSP-coated disk and shoe pin and (b) disk with a coat of ATSP+20% MPCM mixture.

**Table 1** Compositions of the coatings under examination (unit: wt%).

Label	ATSP powder	MPCM powder	PTFE powder
Coating A0	100	0	0
Coating A1	95	0	5
Coating A2	90	10	0
Coating A3	80	20	0

as this is the optimum concentration in ATSP+PTFE blends that yields the best tribological performance, as suggested by the vendor. Also, an increased PTFE concentration brings complexity to the deposition process with negligible favorable effects on the tribological performance.

ATSP is a thermoset polymer with a glass transition temperature of 238  $^{\circ}\text{C}$ , an onset degradation temperature of approximately 400  $^{\circ}\text{C}$  [3], and a curing temperature of 260  $^{\circ}\text{C}$  in the coating format [16]. ATSP has proven tribological performance in a wide range of operational conditions [12, 13, 16–18], and therefore it served as the polymeric matrix in the present study. The ATSP powder (NOWE C100) was purchased from ATSP Innovations Inc., and some of the mechanical properties provided by the vendor of neat ATSP (Coating A0) are presented in Table 2. The MPCM along with the corresponding PCM was purchased from Microtek Laboratories Inc. The used MPCM was Nextek 43D (melting point: 43  $^{\circ}\text{C}$ ), which is a dry powder (> 97% solids) with an average particle size of 15–30  $\mu\text{m}$ . The PCM was paraffin wax, and it was the same material as the core material of MPCM. Figure S1 in the ESM shows the scanning electron microscopy (SEM) images of the MPCM capsules dispersed on a double-face carbon tape, which they varied slightly in diameter. Figure S1(b) in the ESM shows a high-magnification SEM image of a capsule with a diameter of ca. 20  $\mu\text{m}$ . The PTFE powder (Zonyl MP1300) with an average particle size of 12  $\mu\text{m}$  was purchased from Chemours Company.

**Table 2** Mechanical properties of Coating A0 provided by ATSP Innovations Inc.

Tensile strength (MPa)	Compressive strength (MPa)	Hardness (MPa)	Elastic modulus (GPa)
95	303.8	200.0	4.2

## 2.2 Physicochemical characterization of tested MPCM

Several characterization techniques were implemented to measure the physical and chemical properties of the microcapsules. The Fourier-transform infrared spectroscopy (FTIR) was used to detect the functional groups present in the microcapsule. The FTIR spectra were recorded on an infrared spectrometer (IR Prestige-21, Shimadzu) equipped with a diamond attenuated total reflection (ATR) lens.

To analyze the thermal stability and phase transition temperatures, the differential scanning calorimetry (DSC) analysis was conducted using a differential scanning calorimeter (DSC3/700/1190, Mettler Toledo). Three heating and cooling (10 °C/min) cycles were measured under an inert nitrogen atmosphere, where the heating cycle occurs first. The temperature range recorded was 0–200 °C. To obtain the degradation onset temperature ( $T_d$ ) of the bulk PCM and MPCM, the thermogravimetric analysis (TGA) was implemented. The TGA was performed under an argon atmosphere using a thermogravimetric analyzer (TGA2/1100/464, Mettler Toledo) with a heating rate of 10 °C/min. The data were analyzed using STAR<sup>®</sup> software (version 15.00a, Mettler Toledo).

A scanning electron microscope (JSM-IT200LA, JEOL) was utilized to obtain the morphologies of the coatings as well as the shapes and sizes of the microcapsules following tribological experiments. The composite coatings were sputtered with 5 nm of platinum and palladium to enhance the electrical conductivity of the samples. The same instrument was utilized to obtain the energy-dispersive X-ray spectroscopy (EDS) images.

The surface topographies of the coatings were obtained using a stylus profilometer (Dektak XD, Bruker). A 2 μm tip was used to obtain 150 parallel two-dimensional (2D) profiles with a scan length of 17 mm and an acquisition rate of 1 data point/μm. The profiles were acquired over a 3 mm width, resulting in a total scan area of 17 mm × 3 mm for each coating. The profiles were obtained on predefined locations on the untested and tested coatings. The roughness data of the untested coatings were measured, and the change in the surface topography was used to estimate the volumetric wear. The confocal imaging

was conducted with an integrated three-dimensional (3D) optical profilometer (Lambda), and Gwyddion processing software was used to measure the thickness of each coating.

Note that the precise chemical compositions of the melamine shell and paraffin core of the MPCM used in the present study (Nextek 43D, Microtek Laboratories Inc.) are in proprietary possession of the manufacturing company. Nonetheless, the analyses herein provided critical and useful information about the physicochemical properties of the microcapsules and produced composite coatings.

## 2.3 Coating preparation

All coatings were prepared in the laboratory using the electrostatic spray coating technique. The ATSP powder and associated additive powders were mechanically mixed following the recipes, as given in Table 1. Using an electrostatic spray applicator, the mixture was deposited onto the metallic disk substrate. Five passes of spraying were applied to reach the desired coating thickness. The coatings were all cured at 260 °C for 30 min in a laboratory furnace and allowed to cool under ambient conditions afterwards. The thicknesses of the coatings were measured via the confocal microscopy (DSX500, Olympus), as shown in Fig. S2 in the ESM. Before the deposition process, a small piece of tape (Kapton, DuPont) was placed at the edge of the disk, and was removed after spraying each coating, leaving a small trace of the uncoated substrate. Note that material piled-up was formed right at the edge of the step (the red areas) due to coating accumulation between the coated surface and the tape, and therefore the thickness measurements were taken from places, where the coating was uniform. The thicknesses of the coatings ranged from ca. 25 to 55 μm and the exact values are given in Figs. S2(a)–S2(d) in the ESM. Figure 1(a) depicts a neat ATSP-coated disk and uncoated metal shoe pins. Figure 1(b) shows a disc with a coating of ATSP+20 wt% MPCM mixture. The presence of MPCM contributed to the grayish finish in color in contrast to the dark color of the neat ATSP coating.

## 2.4 Tribological tests

The experiments presented in this study were

conducted by a commercial tribometer (MFT-5000, Rtec). A flat pin-on-disk configuration was implemented to simulate the interfacial contact under industrial applications. All pins and disks were cleaned using isopropanol and dried under ambient conditions prior to testing. A constant normal load of 112 N was applied on the pin, which is equivalent to a nominal contact pressure of 1 MPa (calculated based on flat area of contact excluding the central hole). The disk was rotated at 637 r/min, and the center of the pin was 15 mm off the center of the disk that resulted in a sliding linear velocity of 1 m/s. Unidirectional rotating tests were conducted at room temperature and ambient pressure, where the relative humidity was  $50\% \pm 3\%$ . No external lubricant was used for any of the tests. The near contact temperature (NCT) was measured by a thermocouple that was positioned on the circumference of the pin approximately  $1.5 \pm 0.5$  mm above the contact interface. The *in-situ* friction force was measured, and instantaneous COF was recorded at 1,000 Hz of data acquisition rate. The obtained data were used to illustrate the changes of COF with time as well as calculating the average COF for each coating. A minimum of the two samples of each coating, as shown in Table 1, were produced and tested to assure the repeatability of the process.

### 3 Results and discussion

#### 3.1 Differential scanning calorimetry (DSC)

The DSC experiments were conducted on both bulk PCM and MPCM for three cooling and heating cycles. The results obtained for the third cycle are illustrated in Fig. 2. It can be observed that the endothermic peak (i.e., melting temperature) of the bulk PCM is ca.  $46^\circ\text{C}$ , which is approximately the same for the encapsulated MPCM ( $45^\circ\text{C}$ ). This observation indicates that the effect of the encapsulating material on the melting temperature of the PCM is negligible. However, during the cooling cycle, the exothermic peak (i.e., crystallization temperature ( $T_c$ )) for the bulk PCM exhibited two well-defined separate peaks at the  $T_c = 33$  and  $38^\circ\text{C}$ , whereas the MPCM exhibited a single broader peak with two maxima occurring across a narrower temperature range at  $T_c = 29$ – $32^\circ\text{C}$ . The

presence of the two well-defined peaks for PCM could be attributed to the presence of different crystal forms and different dimensions of crystalline domains, or due to the mixed nature of the PCM used. In the case of MPCM, these peaks were merged forming minor humps. Most importantly to the present study is the observation of the effect of microscopic confinement, leading to changes in the crystallization behavior of MPCM versus that of PCM, yet with confirmation of the melting temperatures remaining comparable, which is the activation point, wherein the PCM undergoes a phase change and could potentially lubricate the interface.

#### 3.2 Fourier-transform infrared spectroscopy (FTIR)

Figure 3 shows the FTIR spectra for both bulk PCM and MPCM. The purpose of the analysis was to obtain the information regarding the chemical composition in terms of functional groups presented in the shell and/or core constituent materials.

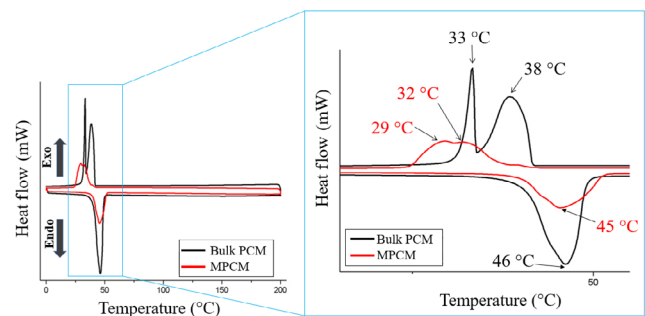


**Fig. 2** DSC curves obtained in the third heating–cooling cycle on bulk PCM and MPCM.

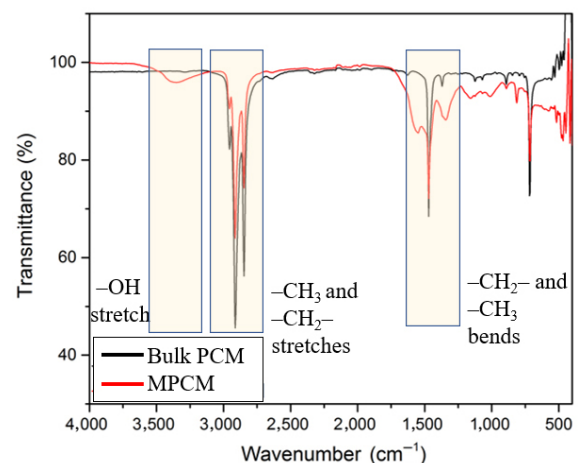


**Fig. 3** FTIR spectra obtained for bulk PCM and MPCM.

Both spectra explicitly show strong peaks related to aliphatic methylene ( $-\text{CH}_2-$ ) and methyl ( $-\text{CH}_3$ ) bends and stretches (ca. 1,450 and 2,800–2,900  $\text{cm}^{-1}$ , respectively). Peaks in these specific regions can indicate the presence of unsaturated alkyl chains commonly found in paraffins, waxes, and oils.

### 3.3 Thermogravimetric analysis (TGA)

The thermal stability of the MPCM is a key factor in the successful embedment of PCM in the form of microcapsules within the polymer matrix. The direct effective embedment of PCMs, such as paraffins in a polymer matrix, with a curing temperature higher than the evaporation/flash temperature of the PCM is impossible. Hence, the role of the encapsulating shell is to provide thermal and physical protection to the PCM to survive the curing process of the polymer matrix. More precisely, the thermal integrity of the encapsulation of the PCM allows for the integration of the PCM into the polymer matrix. The TGA results obtained for both bulk PCM and MPCM are shown in Fig. 4.

The  $T_d$  (i.e., 0.1% mass loss) of the bulk PCM is 81 °C, while encapsulation increases the onset temperature for the MPCM up to  $T_d = 156$  °C. At the curing temperature of the ATSP coating, that is 260 °C, the vast majority of the bulk PCM mass had been lost; however, the MPCM had > 95% mass remaining at 260 °C. This result gives insight to the survival of the microcapsules during the curing process. Additional information that can be extracted from the TGA data

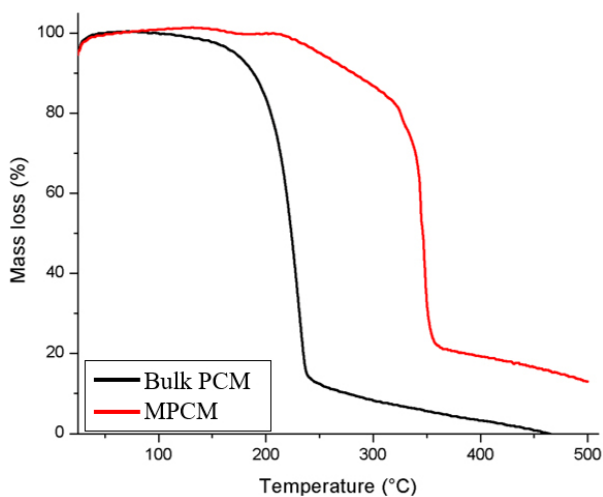


**Fig. 4** TGA results obtained for bulk PCM and MPCM.

is the amount of remaining mass of the MPCM at the ultimate degradation temperature of the bulk PCM. Approximately 18% of the initial mass of the MPCM remains at the complete degradation temperature of the PCM ( $T_f = 465$  °C), which can be attributed to the shell mass. Thus, the core to shell mass ratio is about 4.6.

### 3.4 Surface topography

The surface roughness measurements of the coatings are obtained from the topographical images (Fig. 5) and are listed in Table 3. Figure 5 depicts the 3D topographical images of the as-deposited coatings. The color legend indicates the highest and lowest heights on each coating. All composites exhibit higher roughness compared to the neat coating (Coating A0), regardless of the blending ratio. Coatings A2 and A3 exhibit similar roughness, despite different MPCM contents. Both have increased surface roughness by almost 70%, compared to Coating A0. Knowing that the average size of the microcapsules is comparable to the coating thickness, such trend is expected as they create artificial peaks in the coating topography.

Additionally, the PTFE composite (Coating A1) shows a slightly more uniform topography compared to the MPCM composites (Coatings A2 and A3), which can be attributed to the smaller particle size and potentially better chemical compatibility/miscibility between the matrix and additive. The pin countersurfaces featured a substantially smoother surface with an RMS roughness of 0.1  $\mu\text{m}$ .

### 3.5 Tribological experiments and near contact temperature (NCT)

The *in-situ* COF vs. sliding time ( $t$ ) for each coating is depicted in Fig. 6. The interfacial interactions of the 53100 steel pin against Coating A0 yielded severe fluctuations in the *in-situ* COF, whose amplitude gradually increased with  $t$ . Blending PTFE with ATSP (i.e., Coating A1) clearly altered the contact dynamics of the tribo-pair, demonstrated as a significant reduction in both the fluctuations of the COF as well as the instantaneous COF values. Despite the reduction in the *in-situ* COF, the moving average was increased as the test progressed. PTFE is one of the most commonly used friction reducing solid additives and is widely

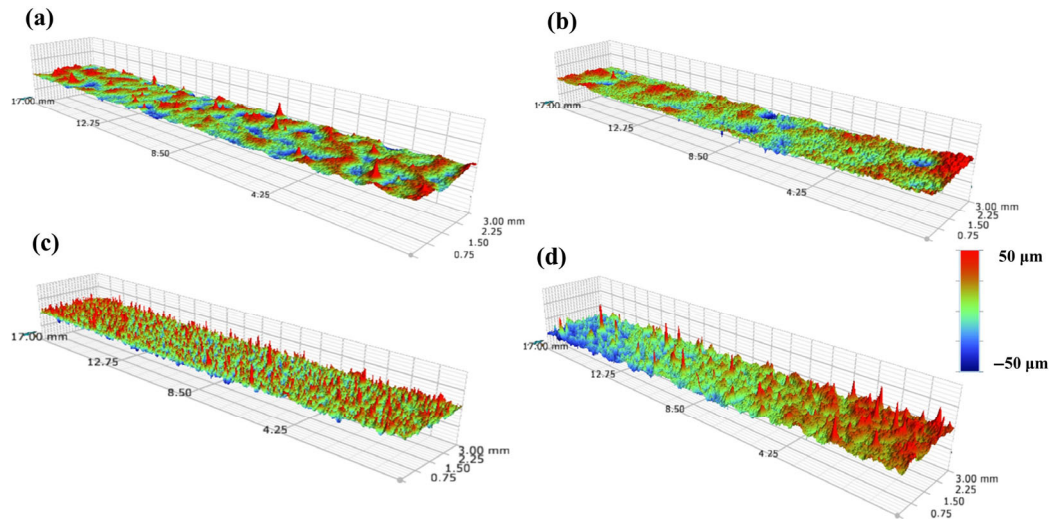


**Fig. 5** 3D topographical images (17 mm × 3 mm) obtained on untested Coatings (a) A0, (b) A1, (c) A2, and (d) A3.

**Table 3** Arithmetic roughness ( $R_a$ ) and RMS roughness of the as-deposited Coatings A0–A3.

Label	$R_a$ ( $\mu\text{m}$ )	RMS roughness ( $\mu\text{m}$ )
Coating A0	1.71	2.22
Coating A1	2.25	2.92
Coating A2	2.87	3.76
Coating A3	2.87	3.80

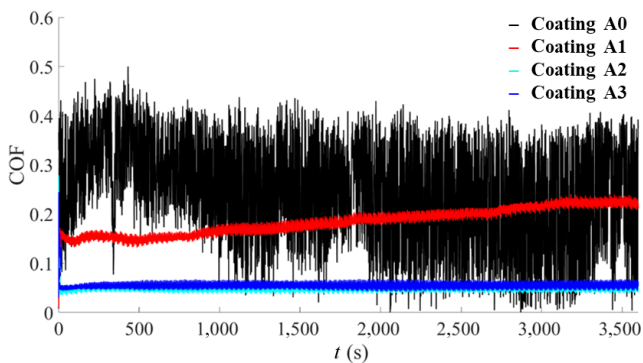


**Fig. 6** Typical *in-situ* COF vs.  $t$  for the coatings produced for the present study.

utilized in polymer composites. Coatings A2 and A3 exhibited the most dramatic changes in the frictional behavior with the presence of MPCM; there was a decrease in the COF, and undesired fluctuations in the *in-situ* COF were substantially suppressed. Moreover, the stability of the COF is striking and resembles a frictional behavior of a fully hydrodynamic contact rather than a dry contact in boundary lubrication.

The average value±one standard deviation of the *in-situ* COF values of identical experiments are shown

in Fig. 7. The average COF of Coating A0 was 0.285, which was reduced by 35% in Coating A1 that was leveraged by the presence of PTFE as the additive lubricant. The friction reduction obtained by the MPCM-filled ATSP composites were 82% and 80%, represented by Coatings A2 and A3, respectively, compared to that of the neat ATSP coating. Therefore, the maximum friction reduction efficacy obtainable by this MPCM was already achieved by the 10 wt% blending ratio, and doubling the MPCM concentration to 20 wt% did not further reduce the COF. The COF oscillations were also reduced by 74%, 95%, and 95% for Coatings A1, A2, and A3, respectively, when compared to COF oscillations measured for Coating A0.

Figure 8 shows the average NCTs measured on the

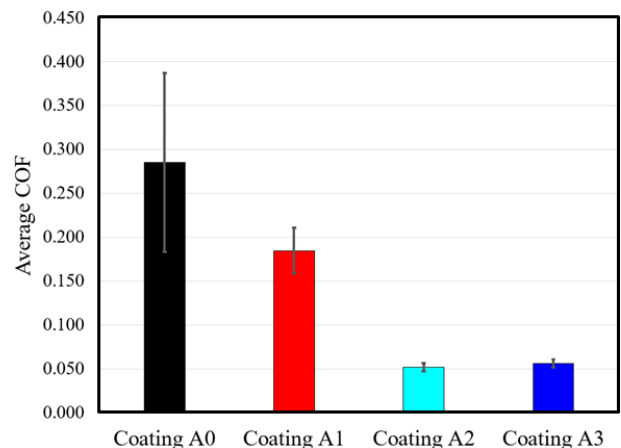


**Fig. 7** Average COF values obtained for the coatings produced in the present study.

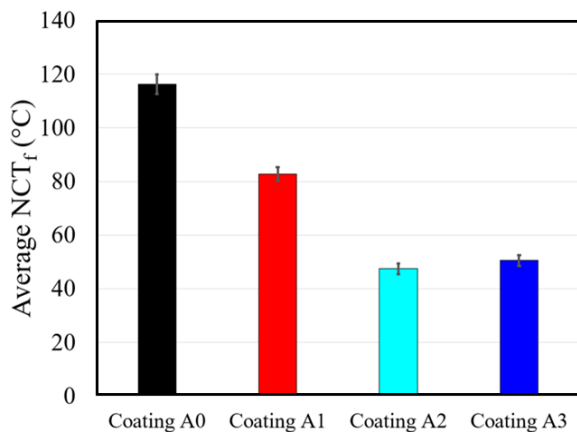


**Fig. 8** Average NCTs obtained from the pins used against Coatings A0–A3.

pins for each tribo-pair. The error bars indicate  $\pm 1$  standard deviation. Lower NCT promises lower thermal softening of the polymer and hence the reduction of hardness degradation of polymers. Hardness is a key parameter in abrasive wear, and therefore Coatings A2 and A3 are expected to exhibit better wear performance.

The 3D topographical images of the wear track of Coatings A0–A3 after the tests were obtained and depicted (Fig. 9), which is the slice of the coatings that straddle the wear track. The wear was uniform on the coatings; thus, this slice is a good representative of the whole wear track. The obtained topographies vividly display the role of the additives in reducing the wear intensity of the neat polymer. Due to excellent wear resistance of MPCM-filled ATSP coatings, it was not possible to obtain a reliable wear coefficient for

the composite coatings, that is, the interface only exhibits mild asperity burnishing and “zero” wear. However, for the neat ATSP and PTFE-filled ATSP (Coatings A0 and A1), the volumetric wear rate [19] was calculated as  $8 \times 10^{-5} \pm 2 \times 10^{-7}$  and  $3 \times 10^{-6} \pm 3 \times 10^{-7}$   $\text{mm}^3/(\text{N}\cdot\text{m})$ , respectively. PTFE provided excellent wear resistance to neat ATSP coating; however, the wear protection that the buffer layer of partially liquid paraffin in the MPCM-filled coatings outperformed that of the PTFE filler.

### 3.6 Scanning electron microscopy/energy-dispersive X-ray spectroscopy (SEM/EDS)

The PTFE friction reduction mechanism in composite polymers has been extensively studied. PTFE generates a thin tribo-film on the counter metallic surface under certain operating conditions, which reduces adhesion and provides low shear at the sliding interface. Subsequently, provided that a uniform and stable film prevails at the interacting surfaces, the frictional force and COF reduce. However, such enhancements are limited by operating conditions and can diminish as the test continues. The lubrication mechanism provided by Coating A1 is through film transfer, which is rich in fluorine and is documented in Refs. [2, 13, 16].

As shown in Fig. 10, the microcapsules were distributed in the coatings and were also exposed on the surface. The SEM images were obtained on the top surface of the wear track of Coating A2. Intact microcapsules were positioned on lower topographies,

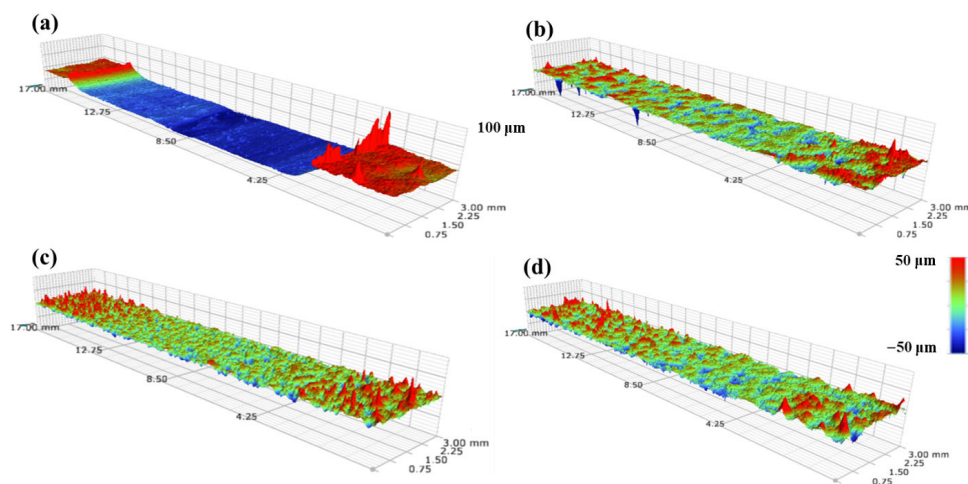


**Fig. 9** 3D topographical wear scans of Coatings (a) A0, (b) A1, (c) A2, and (d) A3 straddling the wear tracks obtained after each test.



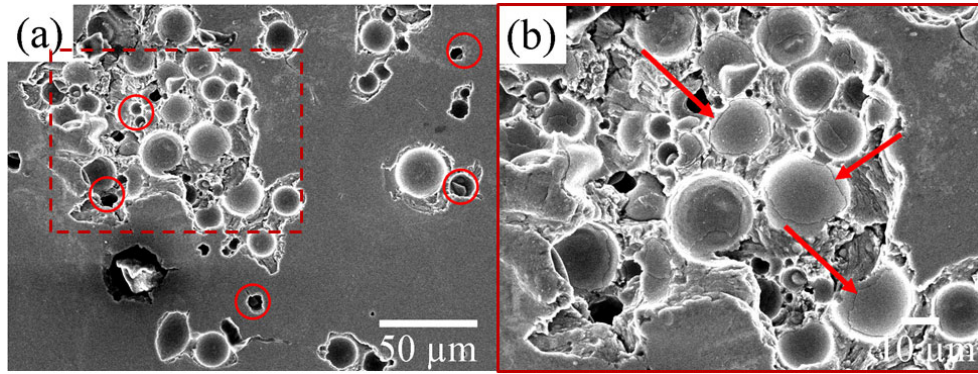


**Fig. 10** (a) SEM image of intact and broken (shown with circles) microcapsules obtained on the wear track of Coating A2 and (b) magnified SEM image showing the cracks (shown with arrows) on the MPCM shell.

while the broken microcapsules (indicated by the circles) had been in contact with the sliding countersurface, resulting in breakage and subsequent releasing of the PCM material, yielding a low COF. The higher magnification image (Fig. 10(b)) clearly exhibits the crack generated on the shell of several microcapsules (shown with the arrows), which could potentially break open and release the PCM, and therefore the lubrication mechanism of the MPCM-filled coatings is uncoupled.

It is hypothesized that the shell of the microcapsules on the interface breaks under contact pressure, resulting in exposure of the lubricious paraffin (i.e., PCM core). Paraffin absorbs the frictional thermal energy and undergoes a phase transition from solid to liquid phase. Liquid paraffin is shown to be an effective lubricant especially for polymeric interfaces [20, 21]. The melted paraffin generates a thin lubricious film that hinders the solid–solid contact and transforms the contact dynamic to a mixed lubrication regime, which otherwise would operate in a dry boundary regime. Hence the outstanding 82% and 72% COF reduction are obtained for Coating A2 compared to those of neat ATSP and ATSP/PTFE composites, respectively. Another advantage that the tested MPCM provides as an additive is the absorption of the frictional heat generation, thus preventing the degrading of the mechanical properties of the polymer matrix, as a result of the increasing temperature [22]. It is well-known that most polymers have weak thermal conductivity [23] and subsequently suffer from accumulation and localization of frictional heat generated at the sliding interface. MPCMs distributed

in the polymer matrix can absorb a fraction of the frictional heat or the environmental heat to undergo phase transition from the initial solid state to a liquid state. More importantly, the markedly lower friction due to enhanced lubrication results in lower frictional heat generation, which is directly correlated to the COF [24].

To investigate the wear mechanisms further, the SEM images of the wear tracks of Coatings A0, A1, and A2 were obtained, as shown in Fig. 11. Coatings A2 and A3 yielded similar tribological behavior, and therefore only the images of Coating A2 were included. The obtained images show that the wear mechanism in neat ATSP is mostly abrasive and fatigue wear, as indicated by crack propagation across the surface (Figs. 11(a) and 11(d)). In case of ATSP/PTFE, localized fatigued zones, where subsurface cracks have reached the surface, are dominant. Further propagation of such cracks can readily generate wear debris, as shown in Figs. 11(b) and 11(e). These observations confirm the findings of Refs. [2, 3, 25] on the wear mechanisms of neat ATSP and ATSP/PTFE composite. In the case of the MPCM-filled composites, the presence of a protective paraffin layer minimized the direct contact of solid asperities, and abrasive wear was prevented (Figs. 11(c) and 11(f)). Weakened areas of the coating, as a result of consumption of the core paraffin, could potentially trigger abrasive wear; however, within the scope of the present study, no such wear was observed.

The EDS analyses on the sliding surface of the 52100 pin countersurfaces provided critical information to support the described lubrication mechanisms. The

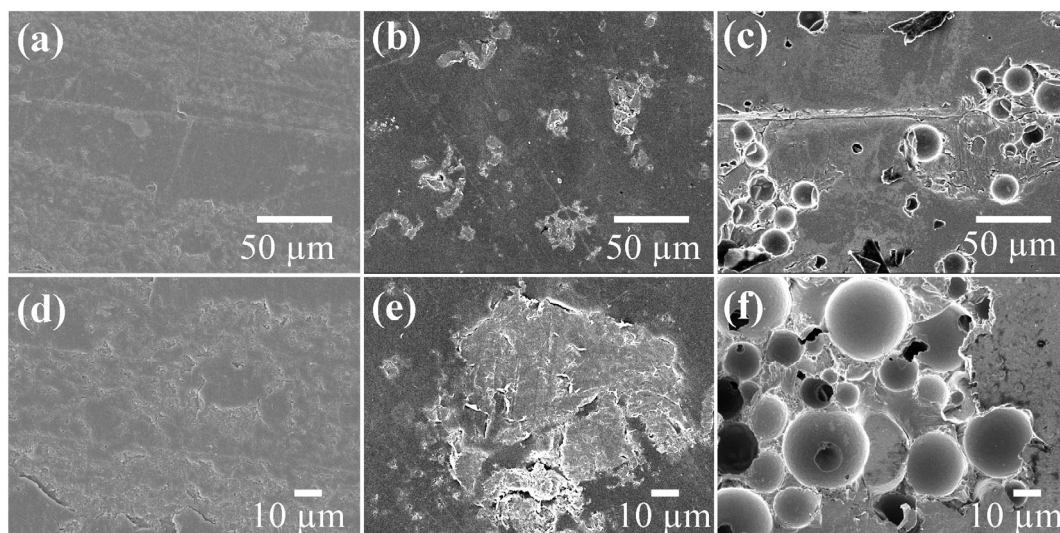


**Fig. 11** SEM images of Coatings (a) A0, (b) A1, and (c) A2 obtained on the wear track and respective higher magnification images showing the surface damage of Coatings (d) A0, (e) A1, and (f) A2.

pin that was tested against neat ATSP was covered by a thick layer of wear debris, which deteriorated the sliding condition by generating excessive heat and adhesion. The effect of the gradual accumulation of compacted wear debris was best demonstrated in the *in-situ* COF behavior of A0 Coating vs.  $t$ , as depicted in Fig. 6. The EDS mappings on a streak of such layer are shown in Fig. 12.

Pins tested against Coatings A1–A3 show no sign of abrasive wear or material compacted on the surface. The EDS analysis of the surface showed a 3.5 at% of fluorine on the pin tested against Coating A1, as shown in Table S2 in the ESM. The presence of fluorine is attributed to the material transfer from the PTFE soft phase of Coating A1. Nevertheless, the amount of material transfer and thereby the wear from the coated surface were not adequate to form compacted stripes or a uniform film on the countersurface. Finally, the pins tested against Coatings A2 and A3

showed an increase in the carbon atomic percentage of approximately 10% compared to a clean, untested 52100 pin sample, for which the EDS results are also provided. Note that only the main elements of 52100 steel were detected from the EDS. Considering the visually unaffected surface of these pins and their coated countersurfaces (Coatings A2 and A3), the origin of such increase could be attributed to the paraffin film that was transferred to the pin surface during sliding.

## 4 Conclusions

We have studied the role of MPCM (paraffin core) as a novel additive for ATSP-based coatings. The MPCM was characterized physically and chemically to obtain the information about its size distribution, chemical composition, and thermal stability. The MPCM was mixed at 10% and 20% mass ratios

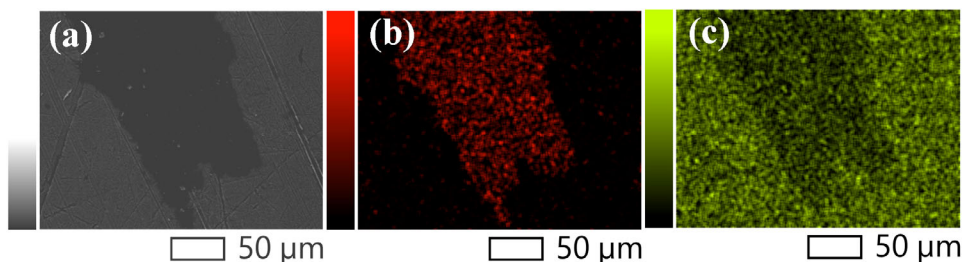


**Fig. 12** (a) SEM image and EDS mappings of (b) carbon and (c) iron on a streak of compacted layer on top of the pin tested against Coating A0.

with ATSP and coated on steel substrates. Coated composites were tested against steel pins under industrial-relevant conditions. To provide a baseline for evaluating the role of MPCM on the tribological performance of the composite, neat ATSP was also coated on steel substrate and subjected to identical tribological testing. Additionally, to demonstrate the superior performance of the MPCM compared to that of the current state-of-the-art industrial additives, PTFE was blended with ATSP at an optimum ratio and was tested under the same conditions. The friction and wear performance of the produced coatings were analyzed and compared, yielding the following conclusions:

1) The COF of the MPCM-filled ATSP (Coating A2) was lower than those of the neat ATSP and PTFE-filled composite by 82% and 72%, respectively.

2) The wear resistance of MPCM-filled coatings within the short duration of the present study was higher than that of ATSP/PTFE coating.

3) The origin of such dramatic enhancement in the tribological performance of the MPCM-filled coatings is attributed to the paraffinic film produced on the metallic countersurfaces, as a result of breakage of the shell and release of the core material of the MPCM.

## Acknowledgements

Fundings of the present study were provided by Texas A&M University X-Grant and by Strategic Transformative Research Program (STRP) Grant, College of Science. The authors also acknowledge the use of the Texas A&M Materials Characterization Core Facility (RRID: SCR\_022202). We gratefully acknowledge the financial support from the Robert A. WELCH Foundation through the W.T. Doherty-WELCH Chair in Chemistry (A-0001). Mariela VAZQUEZ appreciates the support by the National Science Foundation Graduate Research Fellowship Program (Grant No. M1703014). Insightful discussions with Ms. Yidan SHEN are also greatly appreciated.

## Declaration of competing interest

The authors have no competing interests to declare that are relevant to the content of this article.

**Electronic Supplementary Material** Supplementary material is available in the online version of this article at <https://doi.org/10.1007/s40544-022-0733-3>.

**Open Access** This article is licensed under a Creative Commons Attribution 4.0 International License, which permits use, sharing, adaptation, distribution and reproduction in any medium or format, as long as you give appropriate credit to the original author(s) and the source, provide a link to the Creative Commons licence, and indicate if changes were made.

The images or other third party material in this article are included in the article's Creative Commons licence, unless indicated otherwise in a credit line to the material. If material is not included in the article's Creative Commons licence and your intended use is not permitted by statutory regulation or exceeds the permitted use, you will need to obtain permission directly from the copyright holder.

To view a copy of this licence, visit <http://creativecommons.org/licenses/by/4.0/>.

## References

- [1] Friedrich K. Polymer composites for tribological applications. *Advanced Industrial and Engineering Polymer Research* 1(1): 3–39 (2018)
- [2] Nunez E E, Gheisari R, Polycarpou A A. Tribology review of blended bulk polymers and their coatings for high-load bearing applications. *Tribol Int* 129: 92–111 (2019)
- [3] Bashandeh K, Lan P X, Meyer J L, Polycarpou A A. Tribological performance of graphene and PTFE solid lubricants for polymer coatings at elevated temperatures. *Tribol Lett* 67(3): 99 (2019)
- [4] Pan Z H, Wang T C, Chen L, Idziak S, Huang Z H, Zhao B X. Effects of rare earth oxide additive on surface and tribological properties of polyimide composites. *Appl Surf Sci* 416: 536–546 (2017)
- [5] McElwain S E, Blanchet T A, Schadler L S, Sawyer W G. Effect of particle size on the wear resistance of alumina-filled PTFE micro- and nanocomposites. *Tribol Trans* 51(3): 247–253 (2008)
- [6] Bandeira P, Monteiro J, Baptista A M, Magalhães F D. Tribological performance of PTFE-based coating modified with microencapsulated [HMIM][NTf<sub>2</sub>] ionic liquid. *Tribol Lett* 59(1): 13 (2015)
- [7] Khun N W, Zhang H, Yue C Y, Yang J L. Self-lubricating

- and wear resistant epoxy composites incorporated with microencapsulated wax. *J Appl Mech* **81**(7): 071004 (2014)
- [8] Aldousiri B, Shalwan A, Chin C W. A review on tribological behaviour of polymeric composites and future reinforcements. *Adv Mater Sci Eng* **2013**: 645923 (2013)
- [9] Jones M R, McGhee E O, Marshall S L, Hart S M, Uruña J M, Niemi S R, Pitenis A A, Schulze K D. The role of microstructure in ultralow wear fluoropolymer composites. *Tribol Trans* **62**(1): 135–143 (2019)
- [10] Burris D L, Sawyer W G. A low friction and ultra low wear rate PEEK/PTFE composite. *Wear* **261**(3–4): 410–418 (2006)
- [11] Conte M, Igartua A. Study of PTFE composites tribological behavior. *Wear* **296**(1–2): 568–574 (2012)
- [12] Bashandeh K, Tsigkis V, Lan P X, Polycarpou A A. Extreme environment tribological study of advanced bearing polymers for space applications. *Tribol Int* **153**: 106634 (2021)
- [13] Bashandeh K, Lan P X, Polycarpou A A. Tribology of self-lubricating high performance ATSP, PI, and PEEK-based polymer composites up to 300 °C. *Friction* **11**(1): 141–153 (2023)
- [14] Tanaka K, Uchiyama Y, Toyooka S. The mechanism of wear of polytetrafluoroethylene. *Wear* **23**(2): 153–172 (1973)
- [15] Lan P X, Gheisari R, Meyer J L, Polycarpou A A. Surface micro-texturing by hot sintering for advanced bearing polymers for friction reduction under boundary lubrication. *Int J Precis Eng Man* **21**(6): 1025–1034 (2020)
- [16] Lan P X, Gheisari R, Meyer J L, Polycarpou A A. Tribological performance of aromatic thermosetting polyester (ATSP) coatings under cryogenic conditions. *Wear* **398–399**: 47–55 (2018)
- [17] Gheisari R, Lan P X, Polycarpou A A. Efficacy of surface microtexturing in enhancing the tribological performance of polymeric surfaces under starved lubricated conditions. *Wear* **444–445**: 203162 (2020)
- [18] Gheisari R, Polycarpou A A. Effect of surface microtexturing on seawater-lubricated contacts under starved and fully-flooded conditions. *Tribol Int* **148**: 106339 (2020)
- [19] Gheisari R, Bashandeh K, Polycarpou A A. Effect of surface polishing on the tribological performance of hard coatings under lubricated three-body abrasive conditions. *Surf Topogr Metrol Prop* **7**(4): 045001 (2019)
- [20] Jia B B, Li T S, Liu X J, Cong P H. Tribological behaviors of several polymer–polymer sliding combinations under dry friction and oil-lubricated conditions. *Wear* **262**(11–12): 1353–1359 (2007)
- [21] Zhang Z Z, Xue Q J, Liu W M, Shen W C. Effects of lubricating-oil additives on the friction and wear properties of polymers and their composites sliding against steel under oil-lubricated conditions. *J Appl Polym Sci* **76**(8): 1240–1247 (2000)
- [22] Gheisari R, Polycarpou A A. Tribological performance of graphite-filled polyimide and PTFE composites in oil-lubricated three-body abrasive conditions. *Wear* **436–437**: 203044 (2019)
- [23] Huang C L, Qian X, Yang R G. Thermal conductivity of polymers and polymer nanocomposites. *Mater Sci Eng R* **132**: 1–22 (2018)
- [24] Hutchings I, Shipway P. *Tribology: Friction and Wear of Engineering Materials*, 2nd edn. Butterworth-Heinemann, 2017.
- [25] Nunez E E, Yeo S M, Polycarpou A A. Tribological behavior of PTFE, PEEK, and fluorocarbon-based polymeric coatings used in air-conditioning and refrigeration compressors. In: Proceedings of the International Compressor Engineering Conference, West Lafayette, USA, 2010: 1467.



**Reza GHEISARI.** He is currently a display material scientist in Apple Inc, USA. He earned his Ph.D. degree in mechanical engineering from Texas A&M University, USA, in 2019, and his master's degree from Clarkson University, USA,

in 2015. His research interests include tribology of polymers and composite materials with a focus on enhancing the reliability and lifespan of polymeric

materials as more sustainable and cost-effective alternatives for currently available engineering materials. Furthermore, he has a patent on approaching super-lubricity in polymeric coatings using MPCMs such as paraffin microcapsules. In addition, he worked with leading oil and gas companies to develop experimental testing methodologies to mimic the harsh abrasive/corrosive contacts of drilling bits as well as developing novel additives for drilling fluids.



**Mariela VAZQUEZ.** She received her bachelor's degree in science in chemistry from Texas A&M University-Corpus Christi, USA. Then she pursued her Ph.D. degree in organic chemistry from Texas A&M University, USA, under the tutelage of professor Karen L WOOLEY in 2015. Her research focused on synthesizing inverse amphiphilic molecular core-shell bottlebrush polymers to investigate their potential applications in microelectronics and tribology. Specifically, she investigated how varying

the chemical compositions of the core and/or shell block influenced the overall morphological conformation and collapsed or extended configuration of the bottlebrush polymers. She has served on various committees and panels addressing under privileged minority students. She is currently the recipient of the Advancing Career Excellence Scholarship, Texas A&M University Louis Stokes Alliance for Minority Participation Bridge-to-Doctorate (TAMU LSAMP BTD) Fellowship, Texas A&M University Johnson-Aviles Diversity Fellowship, and the National Science Foundation Graduate Research Fellowship (NSF-GRFP).



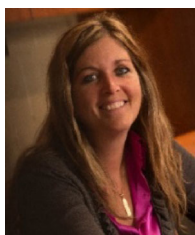
**Vasilis TSIGKIS.** He is currently a Ph.D. student in the MicroTribodynamics Laboratory, J. Mike Walker '66 Department of Mechanical Engineering, Texas A&M University, USA. He received his bachelor's and master's degrees in mechanical

engineering from University of Cyprus, Cyprus, in 2015 and 2017, respectively. His research interests focus on macro-tribological testing and characterization of advanced polymeric coatings, hard diamonds, and superalloys in extreme environmental conditions, including cryogenic and high temperatures for space bearing applications.



**Ali ERDEMIR.** He is currently a professor and Halliburton chair in engineering in J. Mike Walker '66 Department of Mechanical Engineering, Texas A&M University, USA. He earned his master's and Ph.D. degrees from Georgia Institute of Technology, USA, in 1982 and 1986, respectively. In recognition of his research accomplishments, he has received numerous coveted awards and such honors as being elected to the U.S. National

Academy of Engineering, World Academy of Ceramics, and the presidency of the International Tribology Council. He has authored/co-authored more than 300 research articles and 18 book/handbook chapters, co-edited four books, and held 33 U.S. patents. His current research focuses on bridging scientific principles with engineering innovations towards the development of novel materials, coatings, and lubricants for a broad range of cross-cutting applications in energy conversion and utilization systems.



**Karen L. WOOLEY.** She holds the W.T. Doherty-WELCH chair in chemistry and is a university distinguished professor at Texas A&M University, USA, now. She studied at Oregon State University, USA, (bachelor's degree, 1988) and Cornell University, USA (Ph.D. degree, 1993). The first sixteen years of her independent academic

career were spent at Washington University (St. Louis), USA, and she then relocated to Texas A&M University, USA, in July 2009. In addition to her academic positions, she is the co-founder and president of Sugar Plastics, Limited Liability Company, and chief technology officer of Teysha Technologies Ltd. Her research interests include the synthesis and characterization of degradable polymers derived from natural products, unique macromolecular

architectures, complex polymer assemblies, and well-defined nanostructured materials. She has designed synthetic strategies to harness the rich compositional, regiochemical, and stereochemical complexity of natural products for the construction of hydrolytically-degradable polymers, which have impact towards sustainability, reduction of reliance on petrochemicals, and production of biologically-beneficial and environmentally-benign natural products upon degradation—These materials are expected to impact



**Andreas A. POLYCARPOU.** He is currently the James J. CAIN chair in mechanical engineering at Texas A&M University, USA. He received his Ph.D. degree in mechanical engineering from the State University of New York at Buffalo, USA, in

1994. His research interests include tribology, micro/nanotribology, nanomechanics, microtribodynamics,

the global issue of plastic pollution and address challenges resulting from climate change. Her recent awards include election as a fellow of the American Academy of Arts and Sciences (2015), National Academy of Inventors (2019), American Association for the Advancement of Science (2020), the American Institute for Medical and Biological Engineering (2020), and National Academy of Sciences (2020); she was also named as the 2021 Southeastern Conference (SEC) Professor of the Year.

thin solid films, and advanced interface materials. Emphasis has been on micro/nanoscale contact problems with applications to micro-devices, as well as the tribology of devices for reduced energy and improved environmental-related impact. Applications include magnetic and energy storage devices, air-conditioning and refrigeration compressors, nuclear reactors, oil and gas applications, and space applications.